FLOW THROUGH POROUS MEDIA FOR A NOVEL CVD REACTOR

By

ELIAS C. STASSINOS

A DISSERTATION PRESENTED TO THE GRADUATE SCHOOL
OF THE UNIVERSITY OF FLORIDA IN PARTIAL FULFILLMENT
OF THE REQUIREMENTS FOR THE DEGREE OF
DOCTOR OF PHILOSOPHY

UNIVERSITY OF FLORIDA

1989

ACKNOWLEDGEMENTS

First and foremost, I would like to thank Dr. Hong H. Lee for the tremendous inspiration, guidance and support he has provided me during my stay in Gainesville. Without his patience and understanding this dissertation would not have materialized. I would also like to thank Dr. R. W. Fahien, Dr. G. Hoflund, Dr. S. Svoronos, and Dr. P. S. Zory for serving as members of my graduate committee.

Special thanks go to to Rudy Strochscheim and his exceptional ability in glassblowing. He has fabricated all the glassware used in this work. I also thank Tracy Lambert, Ron Baxley, Jim Sharp, and Ed Brown for their help with machining and various other chores in the laboratory. I also thank David Blankenship for taking and developing all the photographs presented in these document.

Finally, I would like to thank all those invisible contributors who have provided me with moral support during this work. My colleagues and friends, Dr. G Lyberatos, Dr. K. Klingman, Dr. J. C. Hong, Dr. I. Toor, Dr. L. Akella, Mr. J. S. Yoo, Mr. V. Coles, Mr. D. Koopman, Mr. S. Cho, Dr. I. Sahinoglou, Mr. Phytos Papathopoulos, Mr. Antonis Vouno Semelithes, Dr. Debboula Ader, and Mr. Reha Uzsoy have made this work possible. I thank my parents and sister for helping me continuously in the good times and the bad times. And the biggest thank you goes to Nienie for being there.

TABLE OF CONTENTS

page

ACKNOWLEDGMENTS ii

ABSTRACT iv

INTRODUCTION 1

THEORY 5

- Reactor Concept 5
- Flow of gases through Porous Media:
  - Single Gas 9
    - Theory 10
    - Experimental 14
    - Results 14
- Flow of Gases through porous Media:
  - Gaseous Mixtures 43
    - Theory 43
    - Experimental 45
    - Results 47
- Reactor Design Considerations 58

EXPERIMENTAL REACTOR 71

CONCLUSIONS AND RECOMMENDATIONS 78

REFERENCES 81

BIOGRAPHICAL SKETCH 83

Abstract of Dissertation Presented to the Graduate School of
the University of Florida in Partial Fulfillment of the
Requirements of the Degree of Doctor of Philosophy

FLOW THROUGH POROUS MEDIA FOR A NOVEL CVD REACTOR

BY

Elias C. Stassinos

August, 1989

Chairman: Dr. Hong H. Lee
Major Department: Chemical Engineering

The concept and design of a novel chemical vapor deposition reactor is presented for epitaxial and nonepitaxial thin film deposition of microelectronic materials. The design of the reactor ensures that a stagnant reactant fluid of uniform concentration is present for the film deposition in the absence of free convection. The source gas is supplied to the reactor by diffusion through a porous inlet section. The reactor should give a better film thickness uniformity and a substantial reduction in the amount of source gas needed for uniform depositon compared to conventional operations.

To model the reactor, the flow of gases through porous media for isobaric low pressure conditions was studied theoretically and experimentally and equations were developed that describe the flux of a single gas or a binary mixture of gases through a porous solid. These equations are valid for all the different regions of laminar flow viscous, transition, and Knudsen. Finally, design equations for the reactor are given and simulations of various reactor configurations are shown.

INTRODUCTION

Thin film chemical vapor deposition (CVD) of epitaxial (monocrystalline) and polycrystalline materials is an integral part of the semiconductor industry. As the electronic devise dimensions continue to shrink and the demand for better understanding and control of CVD processes is increasing, considerable attention is being paid to CVD reactors [Sze (1988)].

Chemical vapor deposition is a process where one or more gaseous species react on a solid surface and one of the reaction products is deposited onto the surface as a grown film.

For example, consider the pyrolysis of Silane (SiH_4) over an epitaxial silicon surface. When a silane molecule strikes the surface, it may be adsorbed or reflected. If it is adsorbed and the temperature is high enough to promote decomposition, the molecule may decompose to Si and H_2. The H_2 is transported back to the gas phase while the silicon left behind builds up a thin solid film. If the thermal energy provided from the surface to the deposited molecules is enough and the surface has a perfect crystalline structure, the deposited molecules realign themselves so that the deposited film has the same crystal structure as the substrate. Otherwise, polycrystalline film occurs or if the temperature is very low the film is amorphous.

The classification of CVD reactors is based on temperature and pressure of operation, and the positioning of substrates and susceptors in the reactors.

Depending upon the shape and placement of the susceptors, CVD reactors are classified as tube wall-flat susceptor, tube wall-tilted susceptor, bell jar-barrel susceptor, pancake reactor, continuous belt and rack type reactor.

CVD reactors are classified as hot-wall or cold-wall depending upon the relative temperature of the reactor walls as compared to the susceptor temperature. In the cold-wall reactor, the susceptor and wafers are kept in the required high temperature, while the reactor walls are maintained cold. The objective here is to cause the desired reaction to take place only on to the hot surface and keep the rest of the reactor free of deposits. To achieve this, RF heating or quartz tungsten halide radiant heaters are used and the susceptors are made up of graphite which couples in an RF field while the reactor is made up of quartz which stays cold. These reactors are mainly used for monocrystalline films because of the better control of impurities that occur due to gas phase nucleation. One of the main problems of the cold wall reactor is that the susceptor temperature is very un-uniform and the growth rate varies according to position on the susceptor. In the hot-wall reactor, however, this problem is eliminated since the reactor is inserted into a furnace and the whole system is maintained at a given temperature. The hot-wall systems are mainly used for non-epitaxial film deposition.

The problem of assuring more uniform depositions was vastly reduced with low pressure operation (LPCVD) because of the better thickness uniformity of a grown film as compared to atmospheric pressure operation (APCVD).

Normally, a reaction is called diffusion controlled if the flux of molecules arriving at the surface is smaller than the rate of molecules reacting so that as soon as a reactant molecule arrives at the surface, it will react to form film. On the other hand, if the rate of reaction is slower than the rate at which the molecules from the gas phase are transported (diffuse) onto the surface, the reaction is said to be diffusion controlled. Although the better uniformity of film grown at low pressure over the APCVD is often attributed to higher diffusivity of the gas at lower pressure, the main reason for the better uniformity has to do with the stabilization of flow in the absence of thermal buoyance effects at low pressures [Westphal (1983)]. The question of which regime (kinetic or diffusion) controls at low pressure is not dependent solely on diffusivity but rather on the relative magnitude of diffusion and intrinsic growth rates which decrease with decreasing pressure.

Although the LPCVD reactor is a significant improvement over the APCVD reactor, it is not without problems. The streamlines intruding into the space between two adjacent wafers mounted on a rack can cause local nonuniformity. In order to achieve uniformity of the films, the flow rate is maintained high so that the reactants are not depleted toward the reactant outlet which means that the amount of gas used used is far in excess of what is needed for the actual film growth. The gases in the semiconductor industry are not recycled because of the impurity problems the recycling can cause. This means that large quantities of very expensive materials are wasted.

In this work, the concept and design of a novel CVD reactor is presented, which can improve the thickness uniformity of a large number of wafers processed, and yet the amount of gas used can be reduced considerably. This reactor would be used for both monocrystalline and polycrystalline film growth.

To model the flow of gases through this reactor it is necessary to understand how gases flow through porous media during nonisobaric conditions at low pressures. The porous media are used in this design as flow distributors. In particular, equations are needed to describe the flux of a gas or a mixture of gases through a porous solid. This equations must be valid in the entire low pressure region. For this, a theoretical and experimental study is presented to derive and verify such equations. Using these equations, modeling of various configurations of the reactor is presented for several typical reaction schemes used in the semiconductor industry.

THEORY

Reactor Concept

Consider a thin film deposition system either polycrystalline or epitaxial. For the polycrystalline case the wafers are mounted on a rack parallel to the direction of flow. The section of the chamber with the wafers is inserted into a heating furnace. For the epitaxial deposition the wafers are placed on a graphite barrel susceptor and the heating is done by an RF heater coil or tungsten halide lamp.

Suppose now that a stagnant fluid medium of uniform concentration and temperature is present throughout the deposition chamber in the absence of buoyancy driven free convection. Suppose also that the gas supplied for the reaction enters the chamber by a diffusion process rather than forced convection of flowing fluid. To ensure the absence of thermal buoyance the reactor must be operated at low pressure. For the gas to enter by a diffusion process, the section between the inlet of the reactor and the part containing the wafers must be separated by a porous medium through which the reactant fluid is transported. This way, the amount of gas used can be made enough to ensure uniform deposition across the wafers thereby reducing substantially the amount of gas used compared to conventional LPCVD reactors. In order to ensure stagnancy of the fluid throughout the reactor the gas must be exiting the deposition section through a porous material. Thus, the reactor must consist of at least five parts: the entrance, diffusion in, deposition chamber, diffusion out, and exit sections.

In accordance with this concept,such a reactor is shown in Figure 1. The porous materials are normal quartz or Pyrex fritted discs, fused onto the reactor or attached by ground fitting joints. The entrance section is maintained at a given pressure by regulating the flow rate of the feed. The gas then is transported through the porous discs whose porosity is chosen to satisfy the reacting chamber needs. The wafers are placed in the deposition chamber and the pressure is maintained at a certain level by adjusting the flow rate and evacuation rate. The reacted gas is then transported through the second porous frit through the exit section which is being evacuated by a pumping system. The pressure in each part of the system depends on the amount of feed and evacuation rate. Notice that if one needs to maintain the pressure of one section at a given level then the pressure at the other sections will be dependent at that value. In other words, the pressure of adjacent chambers is interdependent. The thickness of the porous discs as well as the porosity are important parameters of the design. The smaller the pores are and the thicker the discs, the more difficult it will be for the gas to transport through and the higher the pressure drop will be from section to section. In addition, if the reactant is diluted with the different type of molecules will have different transport rate through the porous material fact which will have to be examined to ensure that proper conditions exist in the deposition chamber.

The wafers must be placed parallel to the flow direction so that if there is any thickness nonuniformity it would be along the wafer dimension and not within wafers. Thus, in principle, anu number of wafers could be processed this way, with limiting factor being the size of the reactor.

In order to describe how the fluid transport is taking place throughout the reactor we must understand first how the gas is flowing through the porous discs. Thus, in the next two sections, the flow of single gases and binary gaseous mixtures will be examined and the overall transport will be discussed.

Flow of Gases through Porous Media: Single Gases

The flow of gases through porous media at low and medium pressures during nonisobaric conditions has been studied experimentally in the past [Adzumi (1937), Carman (1950), Wallick and Aronofsky (1954), Arnell and Hennenberry (1948), Barrer and Barrie (1952), Barrer and Grover (1951), and Grover and Ford (1958)] and various theoretical attempts have been made [Adzumi (1937), Carman (1950), Barrer and Grover (1951), Schwertz (1949), Rigden (1946 and 1947)] to describe the gaseous flux as a function of pressure at the laminar flow region. Unfortunately, no single model can describe the flow in the whole pressure regime (Knudsen,

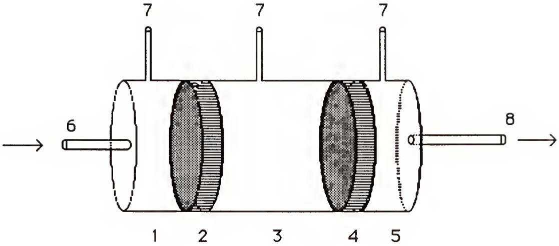

1. Inlet Section
2. Inlet Porous Disc
3. Reaction Chamber
4. Outlet Porous Disc
5. Outlet Section
6. Inlet Port
7. Pressure Measurement Port
8. Outlet Port

Figure 1 Novel Reactor Concept

transition, and viscous) but different equations must be applied to each region. Nevertheless, we are interested in studying the gas phase mass transport through Pyrex fritted discs at pressures below 100 torr to be used as flow stabilizers in LPCVD reactors for epitaxial film deposition.

The flow of gas through porous solid is considered analogous to the flow of gas through capillaries [Carman (1956)]. At high enough pressure, a linear relationship is observed between flow rate and average pressure, and as the average pressure is decreased such that the mean free path of the traveling molecules approaches the size of the pore radius a deviation from linearity is observed. Unlike capillary flows, though, where a minimum is observed [Knudsen (1909), Adzumi (1937 and 1939)], no minimum has ever been reported for porous solids. The net fluid transport is regarded as due to the additive result of molecule-molecule collisions (viscous flux) and molecule-wall collisions (Knudsen flux). In the transition between the Knudsen and viscous regimes where neither dominates, slip is speculated to occur in which the average fluid velocity at the wall is greater than zero. Our goal is to investigate theoretically and experimentally the flow in the Knudsen, transition and viscous regions and formulate an expression for the flow rate that will apply through the whole flow regime. In this section we will concentrate on single gas flow where no diffusive flow occurs. A study of binary mixtures of gases will follow in the next part.

Theory

According to the kinetic theory of viscosity [Chapman and Cowling (1970)], the flow of molecules through a medium takes place due to molecular collisions which give rise to the law of viscosity. The flow rate Q of a given gas is directly proportional to the number of molecules present (pressure) with a proportionality constant μ (viscosity) being independent of pressure. For a porous medium subjected to a pressure gradient dP/dx, where x is the longitudinal path of flow, the flow is described by Darcy's law [Carman (1956)].

$$\frac{Q}{A} = \frac{K}{\mu} P \frac{dP}{dx} \qquad (2\text{-}1)$$

where K is called the permeability coefficient and A is the cross-sectional area through which the transport takes place.

At relatively high pressures (but still in the laminar region) the flux (flow rate per unit area) is linear with respect to average pressure. As the pressure is decreased so that the mean free path is comparable to the pore size, the flux vs average pressure plot is not linear any more. The molecules at low densities collide more and more with the walls and the transport takes place by two mechanisms, molecule-wall and molecule-molecule collisions. Eventually the mean free path becomes so large that the molecular collisions become unimportant and the flow is due to particle collisions with the walls (Knudsen region).

Various models exist to describe the flow in these regions. For the high pressure region Adzumi (1939) adopted a model for the porous medium consisting of a bundle of parallel, uniform, circular capillaries of length L. Using a modification of Knudsen's law of slip through one capillary he derived for the flow of gas through a porous medium the following expression

$$\frac{QPinL}{dP} = \frac{\pi PE}{8\mu} + \frac{2}{3} z\, F\langle v\rangle \tag{2-2}$$

where E, z, and F are characteristic constants of the system adjustable by experiment, P is the average pressure of the system, P_{in} is the inlet pressure, and <v> is the average molecular velocity.

Adzumi's model was modified by Rigden and Arnell (1946 and 1947) and later by Lea and Nurse (1947) and Carman and Allen (1947) who derived the following modified Kozeny equation

$$\frac{QP_{in}L_e}{\varepsilon(dP)L} = \frac{m^P P}{k_0 \mu L_e} + \frac{4rm}{3kL_e}\langle v\rangle \tag{2-3}$$

where m, k, and k_0 are constants of the system , r is the average pore radius, and ε is the void space of the porous medium.

For Knudsen flow, a Knudsen type permeability factor is defined as [Pollard and Present (1948) and Hiby and Pahl (1952)]

$$B = \frac{QP_{in}L}{dP} = \frac{4f_0}{3k}\varepsilon m\langle v\rangle \tag{2-4}$$

which is not easy to asses due to lack of experimental data. Here k, f_0, and m are constants of the system, and ε is the void fraction.

These models have a very limited range of applicability and the values of the coefficients sometimes vary with pressure, thus they are not adequate for our needs. To derive an equation that covers the whole flow region we will use the principles of the kinetic theory of gases for intermolecular collisions [Levine (1978)]. In viscous flow intermolecular collisions dominate while in Knudsen flow only collisions with the walls are present to contribute to the flow.

The kinetic theory provides expressions of the number of each of the different type of collisions. The frequency of wall collisions N_W in a cylindrical tube is given by

$$N_W = \frac{N_0}{4V} <v> = \frac{PN_0}{4RT} \left(\frac{RT}{\pi M}\right)^{1/2} \qquad (2\text{-}5)$$

where M is the molecular weight of the gas, N_0 is the Avogadro's number, R is the ideal gas constant, and V is the volume of the system. Then, the Knudsen flux through a porous medium F_K by analogy can be considered to be proportional to

$$F_K \sim A\,(dP/dx) \qquad (2\text{-}6)$$

where A is a proportionality constant characterizing the system.

The intermolecular collision frequency is given by

$$N_M = \frac{1}{\sqrt{2}} \pi d^2 \left(\frac{8RT}{\pi M_0}\right) \left(\frac{PN_0}{RT}\right)^2 \qquad (2\text{-}7)$$

where d is the molecular diameter.

Then, the viscous flux F_V can be assumed by analogy to be proportional to

$$F_V \sim BP(dP/dx) \qquad (2\text{-}8)$$

where B is a proportionality constant similar to the Darcy permeability. This equation has the same functionality form as equation (2-1). Integration of (2-8) from P_{in} to P_{out} yields

$$F_V L = \int_{P_{in}}^{P_{out}} BPdP = \frac{1}{2} B(P_{in}^2 - P_{out}^2) \qquad (2\text{-}9)$$

which means that any experimental data should give a linear plot of flux vs pressure square gradient.

From equations (2-5) and (2-7), the ratio of the intermolecular to the total number of collisions is given by

$$\frac{N_M}{N_M + N_W} = \frac{BP}{BP+A} \qquad (2\text{-}10)$$

Equations (2-5) and (2-7) have been derived by assuming that only one type of collisions is present at a given instance and thus they neglect the effect the one has on the other.

Now we assume that the influence the one type of flow has on the other is proportional to the corresponding fraction of collisions that cause that flow. The net flow F_t consists of the added contributions of each flow and throughout the whole region would be given by

$$F_t L = \int_{P_{in}}^{P_{out}} \left(\frac{BP}{A+BP}\right) BPdP + \int_{P_{in}}^{P_{out}} \left(\frac{A}{A+BP}\right) AdP \qquad (2\text{-}11)$$

provided equation (2-10) is correct. If we determine the appropriate functionality form for the collision ratio valid in the whole region then equation (2-11) should be valid for any pressure.

Experimental

To measure the rate of flow of gases through the porous frits an appropriate setup (Figure 2) was devised such that the frits were sealed with inlet and outlet ports as well as ports for pressure measurement. The complete experimental setup is shown in Figure 3. The gases used were all research grade. Vacuum was drawn by a two stage roots blower, capable of evacuating up to 180 CFM. The volumetric flow rates were measured by either electronic flowmeter (FR below 20ml/min) or ball type flow meter (FR above 20 ml/min). The pressure at both ends of the frit was measured by Vacuum General capacitance transducers rated to 10^{-3} Torr. Two different frits were examined, coarse ($r \approx 50\mu$) and medium ($r \approx 10\text{-}15\mu$), and four gases were used: N_2, H_2, He, and CO_2.

Results

The flow rate of H_2, N_2, CO_2, and He through the porous frits is reported in Tables 1-8, together with inlet and outlet pressures. Inlet pressures up to 80 Torr are reported. From these data the plot of FLRT vs $(P_{in}^2-P_{out}^2)/2$ is presented in Figures 4-11. The difference of the square of the pressures was chosen rather than the normally used average pressure P because using P implies that the pressure gradient inside the disc is linear which is not necessarily true. As it is seen in the plots the flow is linear at higher pressures but deviates from linearity as the pressure is reduced toward the molecular regime. The pressure at which deviation starts is higher for the smaller pores. From the linear part (viscous region) we can derive the value of B for each gas and each porosity. Using that value and equation (2-11), we can calculate the values of A for the entire pressure region. The results are shown in Figures 12 and 13. We note that A has an initial value A_0 which is constant for at the lower pressure region and it increases with pressure until it reaches a plateau and remains constant. This pattern is present in all cases. We speculate that the initial value of A_0 represents the region the region in which wall collisions dominate. As the number of molecules increases, the number of wall collisions increases too even though the ratio of wall to total collisions is decreasing because the number of intermolecular collisions is proportional to P^2 while the number of wall collisions is proportional to P. Eventually, a leveling in the number of wall collisions occurs and no more increase takes place with increasing pressure despite the fact that the density is increasing. We determined that the simplest function with which we can describe A is

$$A = A_0 \left(1 + \frac{jP}{1+fP}\right) \tag{2-12}$$

where j and f are constants. Thus equation (2-11) becomes

$$F_t L = \int_{P_{in}}^{P_{out}} \left\{\left(\frac{BP}{A+BP}\right)BP + \left(\frac{A}{A+BP}\right)A\right\}dP \tag{2-13}$$

where A is given by equation (2-12). By numerical integration we determine the corresponding values of j and f (given in Table 2) which provide the best fit of the experimental data. We then relate the parameters A_0, B, j, and f of the model to the molecular parameters and the frit pore radius R_p.

$$B = b_0 R_p{}^3 ß^2/M^{1/2} \quad (2\text{-}14)$$

$$A_0 = A_1 M^{1/2} R_p \quad (2\text{-}15)$$

$$j = j_0 ß/M^{1/2} \quad (2\text{-}16)$$

$$f = f_0 R_p \quad (2\text{-}17)$$

We note that f is only a function of the frit porosity. Here, ß is the molecular diameter.

Thus, the total flux of a gas flowing through a porous medium is described by equations (2-13) to (2-17). Equation (2-13) applies to the whole flow region for any gas and any porosity. At low pressure the wall collision term of the equation dominates and it reduces to the Knudsen equation for porous media. At the higher pressure region the first term on the right hand side represents the viscous flux and the second term represents the contribution to the flow due to molecular collisions which is a function of the type of gas and the pore size (the smaller the pore the larger this contribution becomes).

Finally, in Figures 14-17 comparison is made between the model and actual experimental data. The experimentally determined values of the flow rate of each gas is plotted together with the prediction of equations (2-12) and (2-13). The black dotted points are the actual data while the white squares are the calculated values from the model. As it is seen from these plots, the model fits the actual experimental values extremely well. For the majority of points the error is 3% or less. Only for the cases of N_2 and CO_2 through the medium frit the discrepancy between model and experiment is somewhat higher. In all cases though, the maximum deviation is never more than 10%.

Thus, we conclude that we have successfully developed a model that describes the flow of single gases through porous solids based on the principles of the kinetic theory of collisions. In the next section, the case of binary mixtures of gases will be examined.

Flow of Gases through Porous Media: Binary Mixtures

In the previous section of this chapter we have studied the transport behavior of single gases through porous media at low pressures in the presence of pressure gradients. In this part we shall deal with the transport of binary mixtures through the frits in which case pressure as well as mole fraction gradients are present. In this situation, in addition to pure hydrodynamic flow (viscous and Knudsen) binary diffusion takes place and the net flux of each component is the net result of the three simultaneous fluxes. To analyze the situation, binary isobaric diffusion has to be studied to separately to determine the appropriate diffusion coefficients of the gases through the frits and these in turn must be applied to the nonisobaric case.

Theory

In the previous section of this chapter we presented an expression [equation (2-13)] which describes the flow of single gases through porous media during nonisobaric low pressure conditions through the whole low pressure region (viscous, transition,

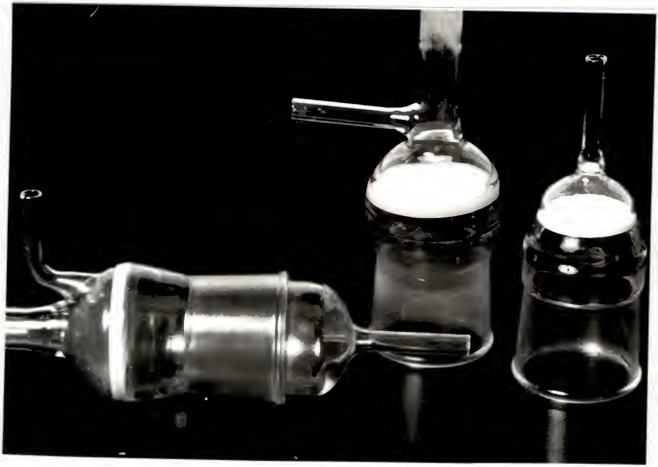

Figure 2 Frit Arrangements

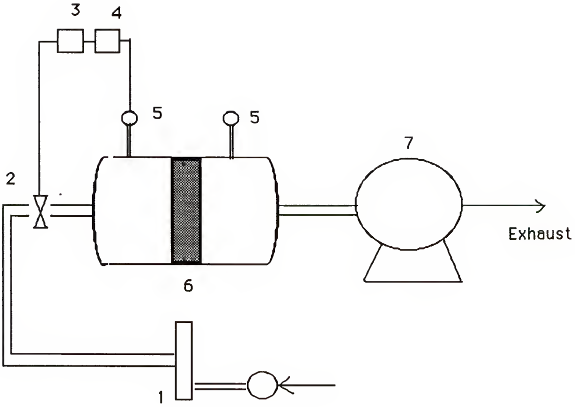

1. Flow Meter
2. Solenoid Valve
3. Pressure Control
4. Pressure Display
5. Pressure Transducer
6. Fritted Disc
7. Vacuum Pump

Figure 3. Experimental Setup For Flow Measurement

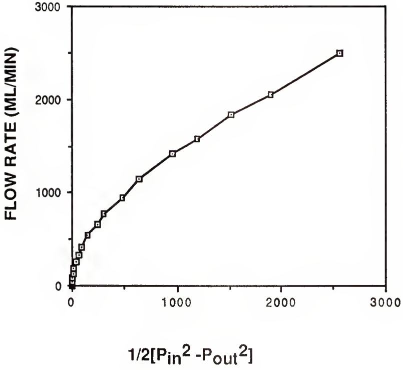

Figure 4 Flow of Gases through Porous Media.
Gas: Helium
Medium Frit

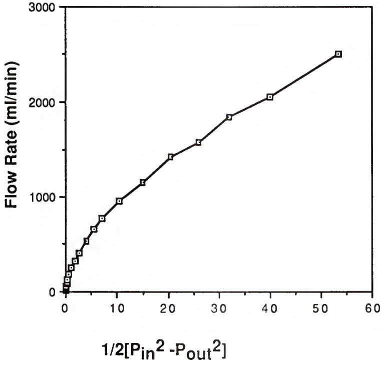

Figure 5 Flow of Gases through Porous Media
Gas: Helium
Coarse Frit

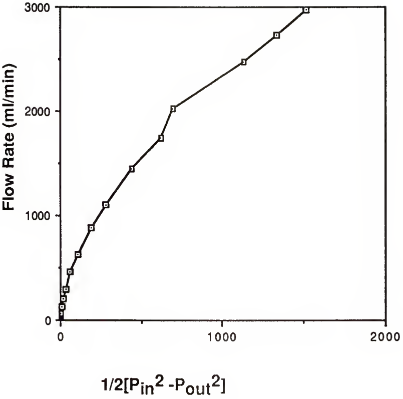

Figure 6 Flow Of Gases through Porous Media
Gas: Hydrogen
Medium Frit

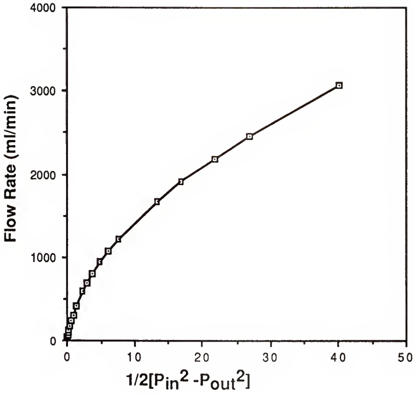

Figure 7 Flow of Gases through Porous Media
Gas: Hydrogen
Coarse Frit

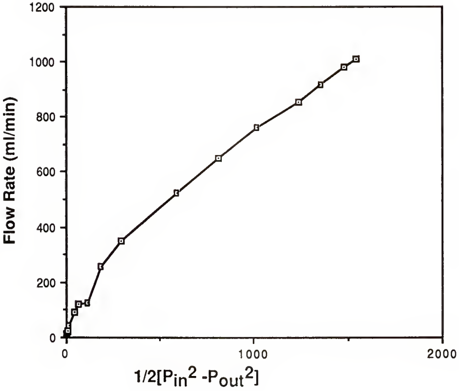

Figure 8 Flow of Gases through Porous Media
Gas: Nitrogen
Medium Frit

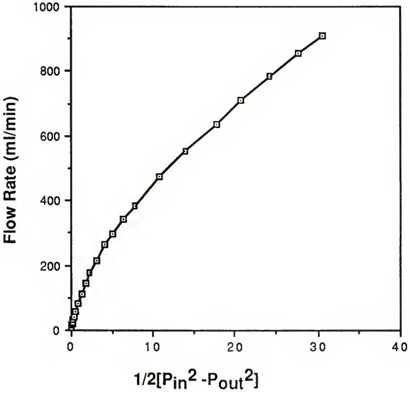

Figure 9 Flow of Gases through Porous Media
Gas: Nitrogen
Coarse Frit

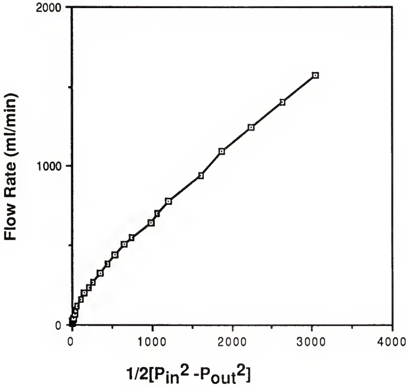

Figure 10 Flow of Gases through Porous Media
Gas: Carbon Dioxide
Medium Frit

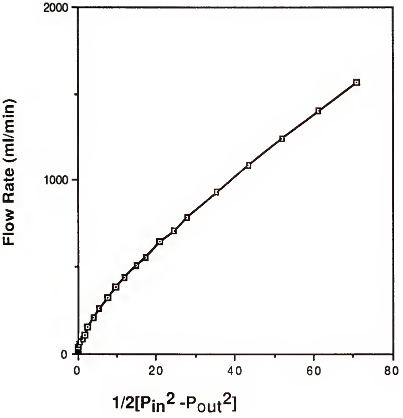

Figure 11 Flow of Gases through Porous Media
Gas: Carbon Dioxide
Coarse Frit

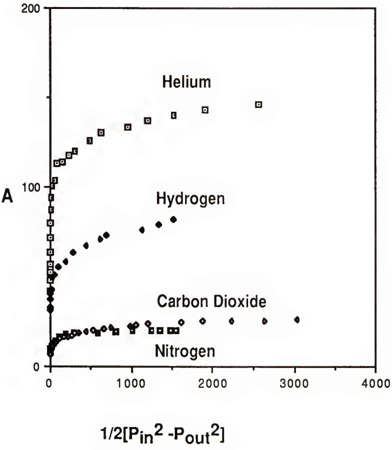

Figure 12 Plot of A vs. Pressure Function
Medium Frit

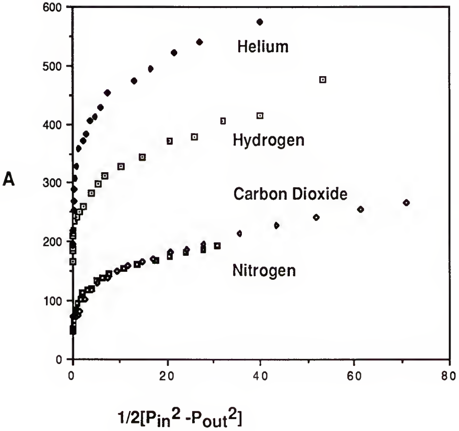

Figure 13 Plot of A vs Pressure Function
Coarse Frit

Table 1 Flow Measurements

Medium Frit
GAS: Helium

P_{in}(Torr)	P_{out}(Torr)	FLRT(ml/min)	$1/2(P_{in}^2 - P_{out}^2)$
71.53	1.38	2500.	2557.
61.66	1.18	2051.	1900.
55.09	1.06	1839.	1517.
48.91	0.97	1584.	1196.
43.61	0.88	1416.	951.
35.64	0.77	1148.	635.
30.89	0.69	952.	477.
24.55	0.59	769.	301.2
21.93	0.54	661.	240.
17.23	0.47	541.	148.
13.20	0.40	412.	87.
10.48	0.36	331.	54.9
8.22	0.32	259.	33.7
5.83	0.26	188.	17.
3.95	0.21	129.	7.78
2.28	0.16	80.	2.59
1.60	0.14	49.6	1.27
1.16	0.12	36.2	0.67
0.95	0.10	28.1	0.45
0.82	0.08	23.8	0.33
0.69	0.07	19.5	0.23
0.55	0.06	12.6	0.15
0.46	0.05	6.3	0.10

Table 2 Flow Measurements

Coarse Frit
GAS: Helium

P_{in}(Torr)	P_{out}(Torr)	FLRT(ml/min)	$1/2(P_{in}^2 - P_{out}^2)$
10.41	1.39	2500.	53.2
9.00	1.19	2051.	39.9
8.09	1.09	1839.	32.1
7.25	0.98	1584.	25.9
6.46	0.90	1416.	20.6
5.40	0.74	1148.	14.9
4.59	0.66	952.4	10.4
3.78	0.55	769.	7.0
3.32	0.51	661.	5.47
2.81	0.46	540.5	3.9
2.27	0.39	412.	2.5
1.87	0.34	330.	1.7
1.49	0.30	259.	1.07
1.12	0.25	189.	0.6
0.82	0.19	129.	0.32
0.66	0.16	105.	0.205
0.53	0.14	80.	0.13
0.38	0.12	51.	0.07
0.28	0.11	37.5	0.034
0.21	0.09	28.1	0.018
0.14	0.06	17.3	0.008

Table 3 Flow Measurements

Medium Frit
Gas: Hydrogen

P_{in}(Torr)	P_{out}(Torr)	FLRT(ml/min)	$1/2(P_{in}^2 - P_{out}^2)$
55.12	2.53	2970.	1515.
51.74	2.42	2728.	1336.
45.57	2.23	2476.	1129.
39.94	1.65	2022.	692.
35.18	1.22	1742.	618.
29.47	0.83	1446.	434.
23.72	0.57	1107.	281.
19.42	0.43	885.	189.
14.29	0.30	629.	102.
10.62	0.23	464.	56.
7.58	0.18	295.	29.
5.29	0.13	199.	14.
3.57	0.09	126.	6.4
2.00	0.06	59.	2.
1.43	0.04	45.5	1.
1.09	0.03	39.	0.6

Table 4 Flow Measurements

Coarse Frit
GAS: Hydrogen

P_{in}(Torr)	P_{out}(Torr)	FLRT(ml/min)	$1/2(P_{in}^2 - P_{out}^2)$
9.23	2.22	3076.	40.13
8.42	1.87	2461.5	27.00
6.72	1.28	2178.	21.76
5.88	1.02	1905.	16.77
5.23	0.86	1667.	13.33
3.92	0.63	1224.5	7.50
3.53	0.56	1076.	6.09
3.12	0.50	942.	4.74
2.78	0.46	800.	3.76
2.45	0.40	690.	2.93
2.16	0.37	588.	2.27
1.67	0.29	417.	1.35
1.34	0.26	312.5	0.86
1.07	0.22	234.	0.55
0.89	0.19	180.6	0.38
0.70	0.16	132.	0.23
0.55	0.13	90.	0.14
0.47	0.12	72.	0.10
0.39	0.10	53.6	0.072
0.27	0.07	41.7	0.03
0.19	0.055	30.	0.016

Table 5 Flow Measurements

Medium Frit
GAS: Nitrogen

P_{in}(Torr)	P_{out}(Torr)	FLRT(ml/min)	$1/2(P_{in}^2 - P_{out}^2)$
55.64	0.51	1010.4	1547.8
54.48	0.50	979.7	1483.9
52.06	0.49	918.4	1355.
49.78	0.47	857.	1239.
45.08	0.42	761.5	1016.5
40.31	0.38	652.	812.4
34.38	0.34	523.4	592.
24.33	0.27	348.	296.
19.25	0.23	256.6	185.
14.95	0.18	127.3	111.7
11.38	0.15	121.2	64.7
9.30	0.14	92.1	43.2
7.01	0.10	42.6	13.62
3.23	0.07	24.8	5.21
2.58	0.055	19.3	3.29
1.73	0.05	15.9	1.5
1.13	0.03	10.74	0.638

Table 6 Flow Measurements

Coarse Frit
GAS: Nitrogen

P_{in}(Torr)	P_{out}(Torr)	FLRT(ml/min)	$1/2(P_{in}^2 - P_{out}^2)$
7.82	0.605	911.	30.6
7.47	0.57	857.	27.7
6.98	0.55	784.	24.2
6.45	0.515	709.	20.65
5.96	0.48	637.	17.65
5.29	0.44	555.	13.9
4.66	0.39	475.	10.8
3.93	0.35	385	7.7
3.56	0.325	342.	6.3
3.20	0.30	299.	5.1
2.86	0.275	266.	4.1
2.49	0.24	213.	3.1
2.13	0.22	177.	2.24
1.89	0.21	145.	1.76
1.55	0.18	111.	1.19
1.29	0.165	84.	0.82
1.01	0.13	59.	0.502
0.84	0.12	43.	0.35
0.69	0.10	32.	0.206
0.57	0.085	25.4	0.16
0.45	0.06	19.3	0.10
0.31	0.05	14.7	0.047
0.22	0.04	10.3	0.023

Table 7 Flow Measurements

Medium Frit
GAS: Carbon Dioxide

P_{in}(Torr)	P_{out}(Torr)	FLRT(ml/min)	$1/2(P_{in}^2 - P_{out}^2)$
77.95	0.75	1569.	3040.
72.61	0.69	1403.	2636.
66.78	0.625	1240.	2230.
61.28	0.56	1092.	1878.
55.40	0.51	938.	1618.
49.	0.44	784.	1200.
46.	0.415	710.	1057.7
42.90	0.38	648.	985.
38.70	0.35	556.	752.
36.35	0.335	509.	661.
32.65	0.31	442.	533.
29.50	0.275	383.	436.
26.45	0.255	326.	350.
22.65	0.215	266.	256.6
20.85	0.20	239.	217.
17.73	0.175	199.	157.
14.93	0.145	163.	112.
11.53	0.125	114.	66.
9.16	0.105	89.	42.
7.13	0.09	65.	26.7
4.52	0.063	38.2	10.
3.92	0.056	33.	7.7
3.20	0.055	26.5	5.1
2.83	0.042	23.5	4.
2.38	0.04	18.2	2.8
2.11	0.035	12.4	2.4

Table 8 Flow Measurements

Coarse Frit
GAS: Carbon Dioxide

P_{in}(Torr)	P_{out}(Torr)	FLRT(ml/min)	$1/2(P_{in}^2 - P_{out}^2)$
11.94	0.81	1569.	70.95
11.08	0.73	1404.	61.17
10.20	0.665	1240.	51.8
9.34	0.60	1092.	43.44
8.43	0.535	938.	35.37
7.48	0.47	784.	27.9
7.01	0.445	710.	24.5
6.54	0.43	648.	20.8
5.88	0.38	555.	17.21
5.47	0.365	509.	14.9
4.87	0.32	442.	11.7
4.40	0.295	383.4	9.65
3.88	0.26	322.6	7.5
3.30	0.22	265.5	5.42
265	0.195	211.9	3.92
2.25	0.155	154.5	2.52
1.86	0.13	106.4	1.72
1.60	0.12	86.7	1.28
1.20	0.095	68.2	0.72
0.81	0.06	53.2	0.32
0.52	0.05	38.2	0.13
0.43	0.04	30.5	0.09
0.28	0.02	23.5	0.04

Table 9 Parameter Values Derived from Data

Medium Frit

Gas	B	A	j	f
H_2	1.34	26.5	0.29	0.15
He	0.68	30.0	0.56	0.14
N_2	0.48	4.5	0.85	0.17
CO_2	0.41	3.5	1.00	0.20

Coarse Frit

Gas	B	A	j	f
H_2	49.7	177.	1.56	0.6
He	33.9	160.	0.97	0.81
N_2	18.6	47.	1.94	0.6
CO_2	17.2	39.	2.2	0.6

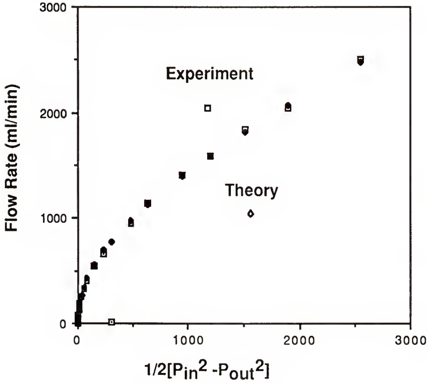

Figure 14 Flow of Gases through Porous Media.
Comparison of Theory and Experiment
Gas: Helium
Medium Frit

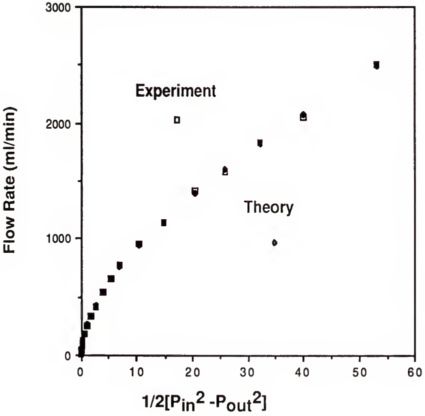

Figure 15 Flow of Gases through Porous Media.
Comparison of Theory and Experiment
Gas: Helium
Coarse Frit

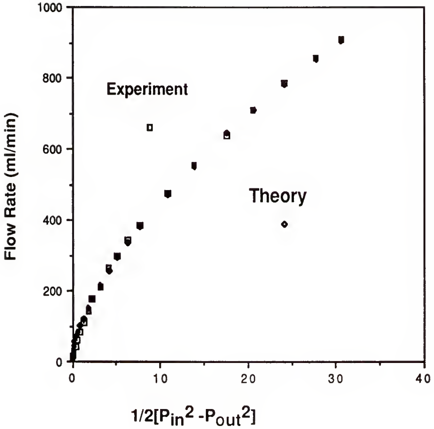

Figure 16 Flow of Gases through Porous Media.
Comparison of Theory and Experiment
Gas: Nitrogen
Coarse Frit

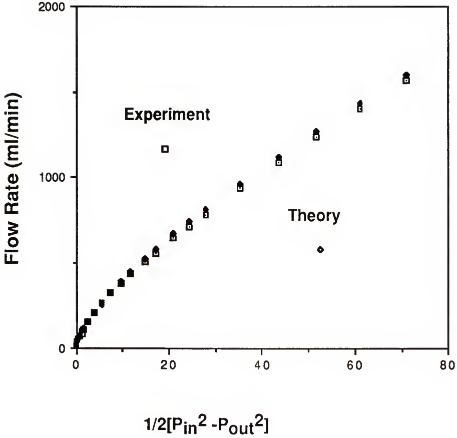

Figure 17 Flow of Gases through Porous Media.
Comparison of Theory and Experiment
Gas: Carbon Dioxide
Coarse Frit

and Knudsen regimes). In the case of mixtures of gases, the situation is more complicated because in addition to the viscous and Knudsen fluxes, ordinary diffusion occurs simultaneously due to mole fraction gradients and the total flow of each component is a additive combination of each fluxes. Thus for a species A the net flux N_{At} is given by

$$N_{At} = N_{Av} + N_{AK} + N_{AD} \tag{2-1}$$

where v denotes viscous, K denotes Knudsen and D denotes diffusional fluxes. The expressions for the viscous and Knudsen fluxes have been discussed in the previous section and it remains to write an appropriate expression for the diffusional flux.

Mason, et al (1963), have derived an equation for the diffusive flux for isobaric transition region diffusion. For binary diffusion of molecules A and B, the fluxes are

$$N_A = \frac{-C_2 D_{AB} k_A}{(K_A + C_2 D_{AB})} RT \frac{dP_A}{dx} + \frac{y_A k_A}{K_A + C_2 D_{AB}} (N_A + N_B) \tag{2-19}$$

and

$$N_B = \frac{-C_2 D_{AB} k_B}{(K_B + C_2 D_{AB})} RT \frac{dP_B}{dx} + \frac{y_B k_B}{K_B + C_2 D_{AB}} (N_A + N_B) \tag{2-20}$$

where C_2 is an effectiveness factor for the porous medium, y_i represents the mole fraction of species i,and D_{AB} is the binary diffusion coefficient. The factors K_i represent the Knudsen diffusion which is considered as a coupled process. Equations (2-19) and (2-20) are valid even when a pressure gradient is imposed across the porous medium. By definition for a binary system

$$P_A = y_A P_t \tag{2-21}$$

$$P_B = y_B P_t \tag{2-22}$$

and

$$y_A + y_B = 1 \tag{2-23}$$

Mason, et al solved equations (2-19) to (2-23) and obtained an expression for the diffusive flux which after proper simplifications for the case where Knudsen diffusion is not considered is

$$N_A = \frac{-C_2 D_{AB}}{[y_A(M - 1) + 1]\, RT} \, \frac{dy_A}{dx} \tag{2-24}$$

where $M = M_A/M_B$.

Equation (2-24) is the contribution of diffusion of component A to the total flux of A [equation (2-18)].

Experimental

The net flow of gaseous mixtures through the porous discs was measured identically as in the case of single gases. The different gas streams were controlled independently so that any mole fraction for each gas could be attained and they were mixed before through the inlet flow control valve. To ensure that steady state conditions existed, a mass spectrometer was used to sample the inlet and outlet sides of the frits during the first few runs and the output was recorded. Two types of frits were studied, medium and coarse, with the following pairs of gases: H_2 - N_2, H_2 - CO_2, He - N_2, and He - CO_2

From these experiments the total flow of the mixture was measured (viscous, Knudsen and diffusive) and since we could not distinguish each type of flow a separate experiment was needed to determine the amount of gas diffusing through the frits and calculate the diffusion coefficients D_{AB}.

For the diffusivity measurements, one of the frits was modified appropriately as shown in Figure 18. Both sides of the frit were sealed by the glassblower to create two cells of equal volume and inlet and outlet ports were added. As far as gases were concerned, N_2 and CO_2 were chosen. A stream of a different gas was passed from each side of the apparatus with equal flow rates passing through each side, and the system was allowed to achieve steady state. The outlets of each side were then passed through a TC gas chromatograph. This system is an adaptation of a diffusion cell. By measuring the flow rates and inlet and outlet concentrations of the gas streams, one can calculate [Lee (1983)] the effective diffusivity of the system from

$$N_A = D_{AB} (y_{Aout} - y_{Ain}) /RT \qquad (2\text{-}25)$$

where N is the flux of the species A and y is the concentration of the gas in the outlet and outlet sides. The value of D_{AB} measured that way is the effective diffusivity of the system and is equal to C_2D_{AB} in equation (2-19), where C_2 is an effectiveness factor which accounts for the tortuous nature of the pores and the amount of void fraction (available cross sectional area for the molecules to transport through). For D_{AB}, the Chapman-Enskog equation [Reid, et al. (1977)] gives

$$D_{AB} = 1.858x10^{-3}\, T^{3/2}\, \frac{[M_A + M_B]^{1/2}}{M_A M_B}\, \frac{1}{P\Omega\partial_{AB}^2} \qquad (2\text{-}26)$$

where Ω is the interaction integral given by the Lennard-Jones potential and ∂ is the collision diameter. From equations (2-25) and (2-26) the value of C_2 can be determined for the particular porous frit, and the value of the effective D_{AB} for the other gases of interest can be determined by substituting the appropriate values of M_A, M_B, Ω, and ∂_{AB} into equation (2-26). The experiments were performed for the medium frit only. For the coarse frit, it was suggested by the manufacturer to assume that the effectiveness factor is twice that of the medium because they have found from their experience with this frits that this is a fairly reasonable assumption that works well.

Results

The value of C2 for the pair N_2 - CO_2 flowing through a medium frit was determined to be 0.11. Thus

$D_{ABeff} = 0.11\ D_{AB}$.

For the coarse frit we approximated the value of C_2 to be 0.2 (twice the value for the medium frit).

The results of the flow of the various gaseous mixtures are shown in Figures 19 - 22 and in Tables 10 - 13. As it is seen, the gaseous mixtures flow through the frits the same way the single gases do , which is something expected because of the fact that the same mechanisms cause the flow. The diffusional process is present as we observed from the diffusion experiments, but it is very small compared to the contributions of the other two mechanisms and even though it affects the flux of each component [equation (2-18)] its contribution to the total flux of the mixture is zero since diffusion is process in which the flow of one component in one direction is counterbalanced by the flow of the other component in the other direction so that the net flow due to diffusion across a plane is always zero. The flow curves for the mixtures linear at the higher pressures (viscous region) and a deviation from linearity is present as the pressure approaches zero (transition and Knudsen regions). The effects of the porosity on the manner in which the mixtures flow are the same as in the single gases, i.e. smaller porosity means higher resistance and consequently higher contribution from Knudsen flow, and the heavier the molecules the slower they flow through the pores.

In order to solve equation (2-18) it is necessary to know the partial pressures of each component in each side of the porous medium, which is something that we have no capability to know. Thus it is impossible for us to solve exactly for the total flux of each component. But if we assume that the contribution of the diffusion process is negligible (something that we observed in our diffusion experiments), then equation (2-18) becomes equation (2-13) for each component. Using these for our mixtures we found that they describe the flow with an error of 10% or less. Thus we conclude that it is a reasonable approximation to neglect the diffusional fluxes and approximate the flux of each component of a binary mixture by equation (2-13).

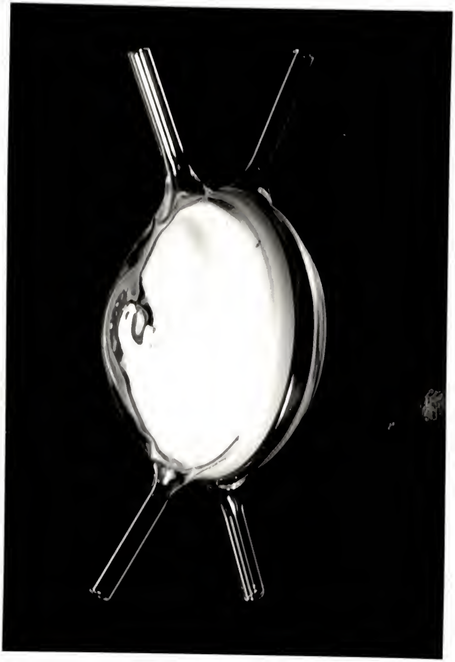

Figure 18 Frit Arrangement for Diffusivity Measurement

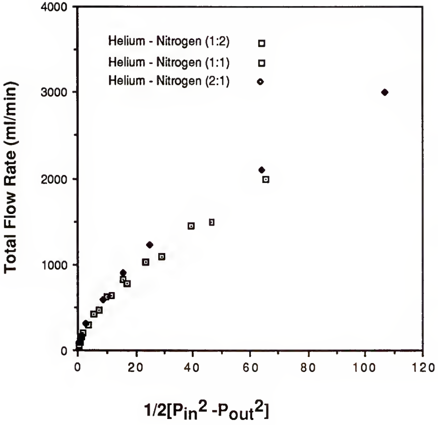

Figure 19 Flow of Gaseous Mixtures through Porous Media
Coarse Frit
Mixture: Helium - Nitrogen

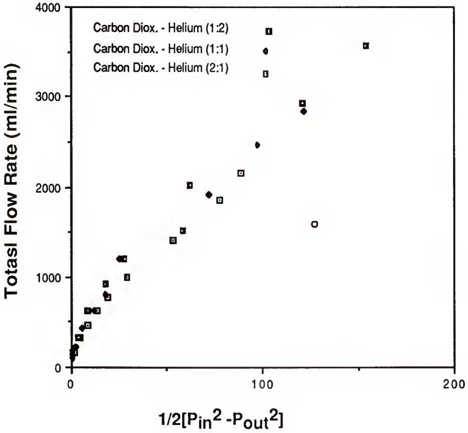

Figure 20 Flow of Gaseous Mixtures through Porous Media
Coarse Frit
Mixture: Helium - Carbon Dioxide

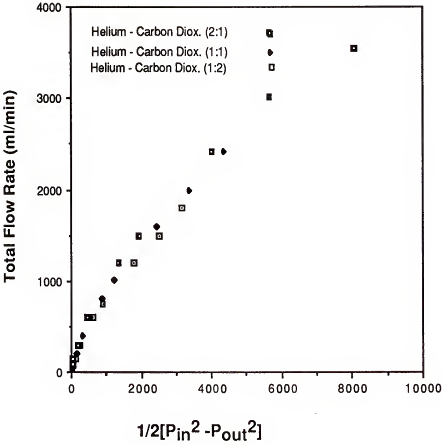

Figure 21 Flow of Gaseous Mixtures through Porous Media
Medium Frit
Mixture: Helium - Carbon Dioxide

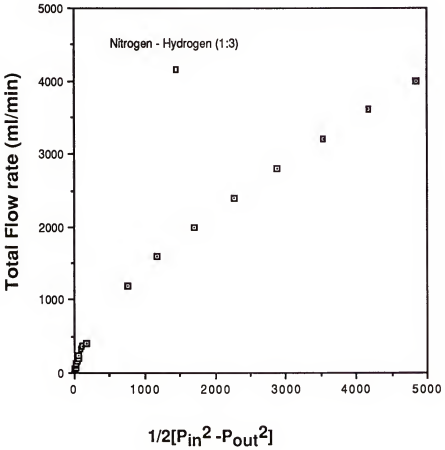

Figure 22 Flow of Gaseous Mixtures through Porous Media
Medium Frit
Mixture: Nitrogen - Hydrogen

Table 10 Flow Measurements for pairs of Gases

Coarse Frit
MIXTURE: He - N_2 (1:2)

P_{in}	P_{out}	FR(He)	FR(N_2)	FR_{total}	$1/2[P_{in}^2 - P_{out}^2]$
9.68	0.86	502	985	1487	46.5
7.69	0.68	342	750	1092	29.3
5.89	0.55	248	530	778	17.2
4.87	0.47	210	430	640	11.8
3.84	0.36	150	320	470	7.3
2.78	0.25	98	205	303	3.8
1.64	0.12	50	101	151	1.3
1.19	0.08	30	61	91	0.7
0.75	0.015	15	32	47	0.3

MIXTURE: He - N_2 (1:1)

P_{in}	P_{out}	FR(He)	FR(N_2)	FR_{total}	$1/2[P_{in}^2 - P_{out}^2]$
11.5	1.08	1004	985	1989	65.5
8.9	0.82	700	750	1450	39.3
6.9	0.65	502	530	1032	23.6
5.6	0.55	400	430	830	15.5
4.5	0.44	301	320	620	10.0
3.27	0.32	210	205	415	5.3
1.89	0.17	98	101	199	1.8
1.36	0.11	60	61	121	0.9
0.83	0.02	30	32	62	0.35

MIXTURE: He - N_2 (2:1)

P_{in}	P_{out}	FR(He)	FR(N_2)	FR_{total}	$1/2[P_{in}^2 - P_{out}^2]$
14.71	1.45	2020	985	3005	107
11.36	1.11	1400	700	2100	64
7.1	0.71	795	430	1225	25
5.6	0.57	600	310	910	15.5
4.09	0.43	394	205	599	8.3
2.42	0.26	209	101	310	2.9
1.65	0.15	116	61	177	1.35
1.00	0.06	61	32	93	0.50

Table 11 Flow Measurements for pairs of Gases

Coarse Frit
MIXTURE: CO_2 - He (2:1)

P_{in}	P_{out}	FR(CO_2)	FR(He)	FR_{total}	$1/2[P_{in}^2 - P_{out}^2]$
13.34	1.10	1451	700	2151	88.7
12.49	0.95	1256	603	1858	77.6
10.35	0.84	907	502	1407	53.2
7.67	0.60	676	320	996	29.2
6.27	0.50	524	248	772	19.5
5.25	0.43	411	209	620	13.7
4.22	0.34	317	148	465	8.9
2.98	0.23	228	98	326	4.4
1.99	0.16	112	50	162	2.0

MIXTURE: CO_2 - He (1:1)

P_{in}	P_{out}	FR(CO_2)	FR(He)	FR_{total}	$1/2[P_{in}^2 - P_{out}^2]$
15.67	1.38	1451	1393	2844	121.8
14.02	1.20	1256	1212	2468	97.3
12.06	1.02	907	1004	1911	72.2
7.2	0.63	524	502	1206	25.7
6.0	0.51	411	394	805	17.9
4.85	0.42	317	301	618	11.7
3.45	0.31	227	210	437	5.9
2.18	0.20	112	107	219	2.4
0.98	0.09	60	51	111	0.5

MIXTURE: CO_2 - He (1:2)

P_{in}	P_{out}	FR(CO_2)	FR(He)	FR_{total}	$1/2[P_{in}^2 - P_{out}^2]$
17.64	1.66	1265	2320	3576	154.2
15.65	1.45	907	2019	2936	121.4
11.17	1.02	676	1350	2026	61.9
10.86	0.88	524	1000	1524	58.6
7.51	0.70	411	793	1204	28.0
6.00	0.58	317	600	917	17.9
4.24	0.41	227	394	621	8.9
2.68	0.28	112	210	322	3.6
1.20	0.12	60	105	165	0.7

Table 12 Flow Measurements for pairs of Gases

Medium Frit
MIXTURE: CO_2 - He (1:2)

P_{in}	P_{out}	FR(He)	FR(CO_2)	FR_{total}	$1/2[P_{in}^2 - P_{out}^2]$
79.2	0.92	1200	603	1803	3136
70.4	0.81	1000	500	1500	2478
59.4	0.68	800	400	1200	1764
42.3	0.48	500	248	748	894
35.5	0.41	400	200	600	630
21.6	0.28	200	98	298	233
14.4	0.20	100	50	150	103.7
7.61	0.11	50	25	75	29
4.74	0.07	30	15	45	11.2

MIXTURE: CO_2 - He (1:1)

P_{in}	P_{out}	FR(He)	FR(CO_2)	FR_{total}	$1/2[P_{in}^2 - P_{out}^2]$
93.1	1.15	1200	1212	2412	4333.1
82.0	1.00	1000	1000	2000	3361.5
69.5	0.84	800	803	1603	2414.8
49.	0.60	500	508	1008	1200.
41.	0.51	400	401	801	840.
24.4	0.36	200	200	400	298.
15.8	0.23	100	98	198	125.
8.2	0.14	50	50	100	33.6
5.1	0.11	30	30	60	13.

MIXTURE: CO_2 - He (2:1)

P_{in}	P_{out}	FR(He)	FR(CO_2)	FR_{total}	$1/2[P_{in}^2 - P_{out}^2]$
191.1	1.62	1200	2350	3550	18258.
106.	1.4	1000	2019	3019	5617.
86.2	1.16	800	1620	2420	3978.
61.9	0.8	500	1000	1500	1916.
51.7	0.7	400	800	1200	1336.
30.1	0.45	200	401	601	453.
18.7	0.3	100	200	300	175.
9.74	0.18	50	98	148	47.4
5.92	0.12	30	60	90	17.5

Table 13 Flow Measurements for pairs of Gases

Medium Frit
MIXTURE: N_2 - H_2 (1:3)

P_{in}	P_{out}	FR(N_2)	FR(H_2)	FR_{total}	$1/2[P_{in}^2 - P_{out}^2]$
98.5	1.55	1000	3000	4000	4850.
91.4	1.43	902	2700	3602	4176.
84.	1.27	800	2405	3205	3527.
75.9	1.12	700	2100	2800	2880.
67.5	0.99	600	1792	2392	2278.
58.4	0.85	500	1500	2000	1705.
48.5	0.7	400	1190	1590	1176.
38.1	0.57	300	899	1199	755.
18.7	0.35	100	299	399	175.
14.8	0.29	90	272	362	109.5
12.7	0.26	80	245	325	81.
10.3	0.24	60	181	241	53.
8.98	0.22	50	150	200	40.5
7.55	0.20	40	120	160	28.5
5.98	0.18	31	90	121	18.
5.13	0.16	27	80	107	13.1
4.33	0.14	20	59	79	9.4
3.02	0.09	15	46	61	4.55
1.89	0.06	10	30	40	1.8

Reactor Design Considerations

Now that we have examined the flow of gases through porous media and we have developed expressions that describe the gaseous flux at any low pressure region in terms of the molecular parameters and porous characteristics, we can model the reactor of Figure 1. for various typical reacting schemes.

The two essential requirements for ensuring uniform deposition in the reactor are uniform concentration throughout the reactor and absence of free convection in the deposition section. For the uniform concentration requirement consider the steady state mass balance in the deposition chamber.

$$A_c(N_{in}-N_{out}) = G_t + D_t = R_t \tag{2-27}$$

where A_c is the open space cross-sectional area of the porous column facing the deposition chamber, N_{in} is the flux of the reactant gas flowing in the reactor, N_{out} is the flux exiting the reaction chamber, G_t is the net growth rate over the total number of wafers in moles/time, and D_t is the deposition onto the reactor walls - if any. If the flux into the reacting chamber is much higher than the total deposition rate R_t, The concentration throughout the chamber should be sufficiently uniform. Rearrangement of equation (2-27) yields

$$1 - \frac{N_{out}}{N_{in}} = \frac{R}{A_c N_{in}} \tag{2-28}$$

Therefore, we can consider the concentration to be uniform within a desired limit if

$$\frac{R_t}{A_c N_{in}} < \partial \qquad (2\text{-}29)$$

where ∂ is a small number (say 0.001 orb 0.1% change in concentration).

For the requirement of no free convection in the chamber consider the core of a stagnant fluid confined between two parallel plates, one at a temperature T_c and one at a higher temperature T_h separated by a distance L [Fahien (1983)]. The criterion for stagnancy is

$$Ra = \frac{L^3(-B_h)(T_h - T_c)g}{v_a} < 1708 \qquad (2\text{-}30)$$

where Ra is the Rayleigh number, $B_h = (-p\, d(1/p)/dT|_p)$ is the coefficient of volume expansion at T_h, p is the fluid density , v_a is the kinematic viscosity, and g is the magnitude of gravity.

Now consider a fluid flowing into the reactor configuration of Figure 1. The gas passes through the porous material into the deposition chamber and from there it exits through the second porous material.If the pressure is low enough, the transport through the porous material will take place by viscous flow, Knudsen diffusion, and molecular diffusion if more than one species is present. The flux equations developed in the two previous sections of this chapte should be applicable in this core, and in the absence of reaction we can write for the flux of species i, N_i

$$N_i = N_{vi} + N_{Ki} + N_{Di} \,. \qquad (2\text{-}31)$$

Substituting equations (2-13) and (2-24) into (2-31) and differentiating we can write the mass conservation equation of each molecular species flowing through each porous column.

$$\frac{d}{dx}\left[\frac{B^2P^2}{A+BP}\frac{dP}{dx}\right]+\frac{d}{dP}\left[\frac{A^2}{A+BP}\frac{dP}{dx}\right]+\frac{d}{dx}(N_{Di}) = 0 \qquad (2\text{-}32)$$

where $A = A_0[1+\beta P/(1+fP)]$ and N_{Di} is given by equation (2-25). At the deposition chamber the following relationship holds

$$P|_{chamber} = P_{ch} = \Sigma\, P_i \qquad (2\text{-}33)$$

where Pch is the total pressure in the deposition chamber. The boundary conditions for the upper column are

$$\Sigma\, P_i = P_{ch} \quad \text{at } x=L \qquad (2\text{-}34)$$

and $P_i/P_{ch} = X_i$ at $x=0$

where X_i is the mole fraction of species i in the feed. The same flux equations apply to both columns and the boundary conditions for the lower column are

$$P_i = P_{out} = 0 \quad \text{at } x_l = L \qquad (2\text{-}35)$$

and $\Sigma\, P_i = P_{ch}$

where we have assumed that the outlet pressure is negligible due to evacuation. If that is not the case a very small value for P_{out} may be used.

The other boundary conditions for solving the conservation equations are the continuity conditions throughout the reactor.

$$N_i|_{x_u=L} = N_i|_{x_l=0} \qquad (2\text{-}36)$$

and $P|_{x_u=L} = P|_{x_l=0}$

The first condition is valid provided the depletion of reactant is negligible [equation (2-30)] holds. The solutions of these equations yields the necessary information needed for the operation of a reacting system. Notice that analytical solutions of these systems of equations are not feasible and numerical techniques must be used to obtain solutions.

Let us now consider some thin film growth cases. First, consider the simple case of polycrystalline deposition of Si using pure Silane feed at around 0.5 to 5.0 Torr with a typical flow rate of 100 ml/min. In this case, only one conservation equation is needed for each porous disc with no molecular diffusion taking place.

$$\frac{d}{dx_u}\left[\frac{B_{Si}^{2}P^{2}}{A+B_{Si}P}\,\frac{dP}{dx_u}\right]+\frac{d}{dx_u}\left[\frac{A^{2}}{A+B_{Si}P}\,\frac{d}{dx_u}\right]=0 \qquad (2\text{-}37)$$

for the upper porous column, and

$$\frac{d}{dx_l}\left[\frac{B_{Si}^{2}P^{2}}{A+B_{Si}P}\,\frac{dP}{dx_l}\right]+\frac{d}{dx_l}\left[\frac{A^{2}}{A+B_{Si}P}\,\frac{dP}{dx_l}\right]=0 \qquad (2\text{-}38)$$

for the lower porous column, with

$$\begin{aligned} P &= P_{in} && \text{at } x_u = 0 \\ P &= P_{ch} && \text{at } x_u = L_u \text{ and } x_l = 0 \\ P &= 0 && \text{at } X_l = L_l \end{aligned} \qquad (2\text{-}39)$$

and $N|_{x_u=L_u} = N|_{x_l=0}$.

Shown in Figures 23 -27 are the results of the simulation for two different reactor arrangements, one reactor arrangement with two "medium" frits and one arrangement with a "medium' at the inlet and a "coarse" at the outlet, all of the same thickness. The effects of the pore diameter on the operating conditions is as follows.

- For a given flow rate and operating pressure (pressure in the deposition section), the inlet pressure is higher for the medium-medium configuration. This happens because the presence of the coarse frit (frit with larger pores) at the outlet of the other configuration creates less resistance to the flow, so that in order for the pressure to be maintained at the same level at the center section with the same flow rate a smaller pressure gradient must exist between the inlet and center sections.
- The outlet pressure will be lower for the medium-medium configuration for the same reasoning.
- For a given inlet pressure and flow rate in the systems the operating pressure will be lower for the medium-coarse configuration because of less resistance to flow.

Let us now consider another example of a typical system commonly used. Very often, the semiconductor gas reactant is mixed with large amounts of inert gas (carrier gas) such as H_2, N_2, or less frequently, Ar. Most often, this is done for safety purposes because the majority of semiconductos source gases are flammable and highly explosive when present pure or in large concentrations. In addition, the presence of the inert sometimes improves the quality of the material grown because it carries away reaction byproducts such as chlorine. Two of the most widely used mixtures of gases for silicon deposition are the SiH_4 - H_2 and SiH_4 - N_2 mixtures with fraction of silane delow 20%. For this case we need to write the conservation equation for each component present in the reactor. For silane we have

$$\frac{d}{dx_u}\left[\frac{B_{Si}^{2}P^{2}}{A+B_{Si}P}\,\frac{dP}{dx_u}\right]+\frac{d}{dP}\left[\frac{A^{2}}{A+B_{Si}P}\,\frac{dP}{dx_u}\right]+\frac{d}{dxu}(N_{Di})=0 \qquad (2\text{-}40)$$

for the upper column, where the diffusion term is given by equation (2-25), and

$$\frac{d}{dx_l}\left[\frac{B_{Si}^{2}P^{2}}{A+B_{Si}P}\,\frac{dP}{dx_l}\right]+\frac{d}{dP}\left[\frac{A^{2}}{A+B_{Si}P}\,\frac{dP}{dx_l}\right]+\frac{d}{dx_l}(N_{Di})=0 \qquad (2\text{-}41)$$

for the lower column.The same equations apply for the carrier gas j.

$$\frac{d}{dx_u}\left[\frac{B_{j}^{2}P^{2}}{A+B_{j}P}\,\frac{dP}{dx_u}\right]+\frac{d}{dP}\left[\frac{A^{2}}{A+B_{j}P}\,\frac{dP}{dx_u}\right]+\frac{d}{dx_u}(N_{Di})=0 \qquad (2\text{-}42)$$

for the upper column, and

$$\frac{d}{dx_l}\left[\frac{B_{j}^{2}P^{2}}{A+B_{j}P}\,\frac{dP}{dx_l}\right]+\frac{d}{dP}\left[\frac{A^{2}}{A+B_{j}P}\,\frac{dP}{dx_l}\right]+\frac{d}{dx_l}(N_{Di})=0 \qquad (2\text{-}43)$$

for the lower column. The boundary conditions are

$P_{Tin} = P_{j\text{-}in} + P_{Si\text{-}in}$ at $x_u = 0$
$P_{ch} = P_{j\text{-}ch} + P_{Si\text{-}ch}$ at $x_u = L$ and $x_l = 0$
$P = 0$ at $x_l = L$
$N_j|_{xu=o} = N_j|_{xu=L} = N_j|_{xl=o} = N_j|_{xl=L}$

and similarily for silane.The results of the simulation are shown in Figures 27 and 28. In the case of Nitrogen (Figure 28) for a total pressre of 10 Torr in the center core and a 10% fraction of silane, the total pressure in the inlet is 25. Torr and the fraction of silane is 12%. In this case the gases flow through the pores very similarily because of the fact that the two molecules have similar size (collision diameter) and the pores exert similar resistance to both.

On the other hand, for tha case of Hydrogen carrier (Figure 27), for a center pressure of 10 Torr and 10% silane fraction, the inlet pressure is 17.5 Torr and the silane fraction is 18%. This is because Hydrogen is a much smaller molecule and it flows more freely through the pores so that a greater partial pressure drop exists between inlet and center for tha larger molecule and thus, a larger mole fraction. This of great interest,and it becomes very important in the cases wher the mole fraction must be maintained below a maximum value fo safety reasons and the selection of porous material must be carefully considered for pore size anmd frit thickness.

Even though frits of different thickness were not available to study directly, it is obvious that the thicker the frit is the higher the resistance to flow would be and consequently the higher the pressure drop would be across a thicker frit.

From the above results it is obvious that the porosity and thickness of the frits used dictate the dynamics of the system. In order for a particular system to be designed, one must solve the appropriate set of conservation equations for a given arrangement to determine the operating conditions. To do this , any two of the pressures need to be specified or one of the pressures and the flow rate.

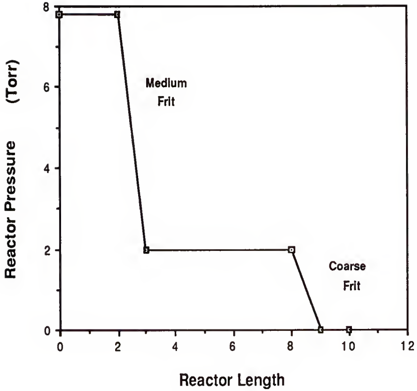

Figure 23 Flow of Silane through CVD Reactor
Medium - Coarse Configuration

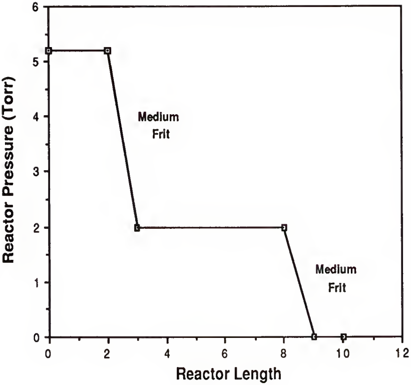

Figure 24 Flow of Silane through CVD Reactor
Medium - Medium Configuration

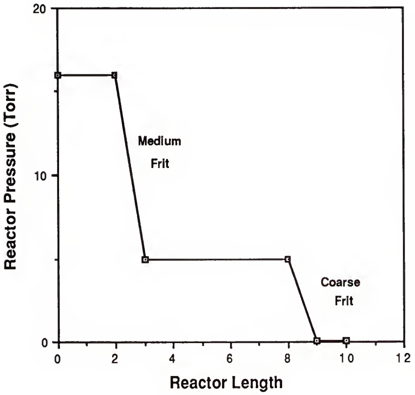

Figure 25 Flow of Silane through CVD Reactor
Medium - Coarse Configuration

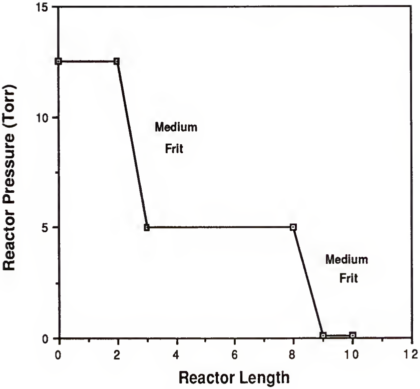

Figure 26 Flow of Silane through CVD Reactor
Medium - Medium Configuration

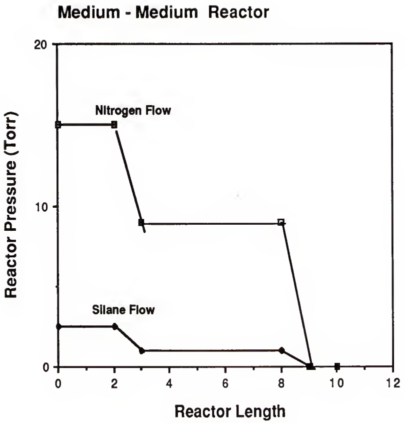

Figure 27 Flow of Silane Mixture through CVD Reactor
Mixture: Silane - Nitrogen
Medium - Medium Configuration

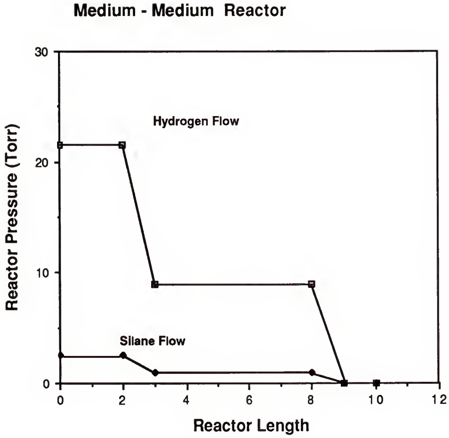

Figure 28 Flow of Silane MIxture through CVD Reactor
Mixture: Silane - Hydrogen
Medium - Medium Configuration

EXPERIMENTAL REACTOR

The experimental part of this work consisted of the design and construction of a reactor that conforms to the requirements of the novel concept as well as some preliminary flow results.

The overall experimental setup is shown in Figure 29. The required equipment are: a reactor with fritted discs, gases a gas manifold, flow meters and flow controllers, a pressure activated control valve with controller, various pressure transducers, a large capacity vacuum pumping system, a scrubber for the gas outlet, susceptors, and heating systems. A detailed description of each part follows.

The reactor was constructed in the glass blowing facilities of our University. The main body of the reactor (deposition chamber) was a fused quartz tube (80 mm diameter) with two 71/60 female quartz ground joints on both sides and a port for pressure transducer attachment. The fritted discs were Pyrex "medium" and "coarse" "KIMBLE' filtration discs attached to 71/60 male Pyrex ground joints with a port for pressure transducer and a inlet port for gas transport.

The pressure in each section of the reactor was measured with Vacuum General capacitance transducers. For the inlet and deposition section the CMLB was used which has an operating range 0.1 - 1,000 Torr. For the outlet, a model CMH was used with a range $1X10^{-4}$ - 1 Torr. It was found that under stable thermal conditions the CMLB models could detect pressure accurately down to 0.01 Torr. The pressure in the deposition chamber was maintained at a given value with a pressure control system. The signal of the transducer was received by a display-power supply (Vacuum General model 80-1). This was connected to a pressure controller (vacuum General model 80-6B) on which the set point was adjusted. The controller actuated a solenoid control valve (Vacuum General model CV2-41 with operating range 0-10,000 sccm).

The pumping system was a two stage Kinney Vacuum roots blower with mechanical roughing pump. The maximum evacuation capability was 180 CFM. The system was equipped with a particulate filter for oil cleaning.

The gas feeding system consisted of gas cylinders, purge assembly, gas regulators, flash arrestors connected in line to the flammable gases, flow meters with flow control valves, and tubing. The source gas cylinder was connected with a purge assembly for cyclic purging purposes on which the regulator was connected. An inert gas line was connected to the purge assembly for dilution and purging purposes. A flash arrestor was connected after the regulator to ensure that in case any flame would be created downstream, it would not travel back to the source gas cylinder when a flammable gas was used. The flow meters and flow controllers were Matheson ball type meters calibrated at standard conditions. To ensure the flow meters was the one used during calibration, the control valve was placed in the outlet of the meter so that the pressure up to the point of the control valve would be the one set from the regulator. The setup was then connected to the piezoelectric valve. The connecting lines were 316 stainless steel heavy wall tubing. The connections were Ultra-Torr Cajun fittings with viton o-rings to ensure leak free conditions.

The outlet gas was passed through a scrubber to ensure that no flammable or toxic material was released in the atmosphere. Water was used as a solute. The exhaust was then vented. The complete setup was installed in a special facility constructed for the handling of pyrophoric gases. A vented enclosure (3 ft. x 14 ft x 8 ft high) was constructed next to the fume hood and the side panel of the hood was removed so that the two enclosures were interconnected. The inside of the enclosure was covered with flame resistant aluminum paint, and a heat activated sprinkler system was installed over the area in which the gas cylinders were to be located. An exhaust fan (850 CFM) was used to ventilate the enclosure. The reactor and pressure control system were placed inside the hood so that the complete setup was continuously vented. A portable hazardous gas leak detector (Matheson model 8057) was used to continuously monitor the laboratory area for leaks.

For thin film silicon deposition experiments, various wafer (susceptors) holders were constructed. For polycrystalline deposition a quartz rack was fabrickated in the glass blowing shop. For epitaxial deposition a number of different shape graphite susceptors were machined to one two two-inch wafers. For cold wall depositions, an RF generator was available (EA Heating 3kw power generator operating at 450 KHz) and various Chromalox radiant quartz tungsten halide lamps for radiant heating.

The reactor was preliminary operated with inert gas (N_2) with the medium-medium and medium-coarse frit arrangement.The results are shown in Figure 30 and 31. As the flow rate increases and the evacuation rate remains constant the pressure in the deposition chamber increases. In addition, for a given inlet pressure the pressure is lower in the deposition chamber for the medium-coarse configuration than for the medium-medium configuration, as expected, since there is less resistance to the flow from the coarse porous frit. This reactor can be operated at any pressure in the deposition chamber.

In addition to the preliminary flow experiments, a flow visualization experiment was performed to observe the gas distribution into the reactor chamber. This was achieved by generating a glow discharge into the reactor chamber. A graphite susceptor was placed in the center of the reactor and the setup was wrapped with an Rf generator coil. The system was evacuated and N_2 was introduced and the pressure was maintained between 0.8 - 1.0 Torr. When an RF field was applied by turning the power of the generator up and the temperature of the susceptor reached 300 C, the gas passing over the susceptor is ionized and plasma is generated. It was found that this occured at a pressure below 12 Torr. but the best visible glow for our purposes occured at 1.0 Torr. Much below that value, the glow was very bright for any flow patterns to be distinguished. With proper arrangement, it was possible to create a visible glow throughout the reactor length and observe the gas flow patterns. This was done for reactors with and without porous discs so that the effect of the presence of the porous discs could be observed. When no porous discs were present the pattern was as follows. In the entrance of the reactor, a thin glowing line was visible at the center of the reactor and continued up to the position of the susceptor. The thickness of that line was approximately the same as the thickness of the inlet port of the reactor. Above the susceptor, the pattern was very diffuse due to the interference of the field with the graphite susceptor. After the susceptor, the thin line was again visible, until the exit port of the reactor and its thickness was approximately that of the outlet port of the reactor. This means that the flow in the reactor is concentrated at the center portion of the tube, where the fluid velocity is maximum) and very little gas is present at the outer parts of the reactor close to the wall. According to the flow pattern observed, if there were wafers positioned axially along the reactor length and if there would be no RF interference, the deposition on this wafers would be maximum at the center line of the reactor and it would decrease along the radial direction provided that an overwhelming amount of gas is not fed into the reactor. This is the reason why nonuniformities are observed along the radial direction in CVD reactors and the flow rate must be raised appropriately to ensure that there is enough gas for the deposition to take place evenly everywhere. Thus, we have concluded that we observed that gas flows nonuniformly along the reactor when no porous frits are positioned.

When two frits were placed at the inlet and outlet of the chamber, the flow pattern was different. The diffuse pattern over the susceptor was still present, but the thin plug type lines along the axial direction from the inlet to the susceptor and from the susceptor to the outlet of the reactor are much less visible. Rather, a much more diffuse pattern is present at the vicinity of the graphite, while almost nothing is visible at the inlet and outlet of the reactor. This gives credence to the concept that placing porous discs at the inlet and outlet of the reactor would create a much better distributed flow along the radial direction of the reactor. It is concluded that a very good distribution of the gas flowing into the reactor through the porous frits takes place and that should considerably enhance the deposition uniformity along the radial direction of the reactor. It remains to perform actual deposition of some thin film to verify the conclusions of the flow visualization experiments.

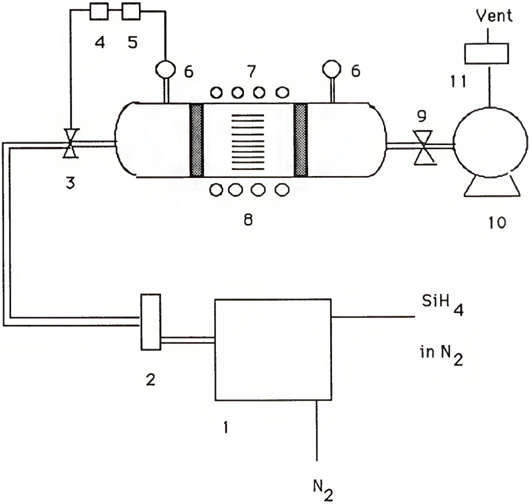

1. Manifold
2. Flow Meter
3. Solenoid Valve
4. Pressure Controller
5. Pressure Display
6. Pressure Transducers
7. Heating Coils
8. Reactor with Wafers
9. Isolation Valve
10. Vacuum Pump
11. Scrubber

Figure 29 Experimental Reactor Setup

CONCLUSIONS AND RECOMMENDATIONS

A novel concept and design has been presented for a CVD reactor for thin film deposition of materials in microelectronic processing. The design ensures that there is a stagnant fluid of uniform concentration throughout the reactor deposition section. This is achieved by placing porous sections in the inlet and outlet of the reactor so that the reactant enters and leaves the deposition section by diffusion through a porous medium rather by forced convection. With this design a better film deposition uniformity along the radial direction is expected and a substantial reduction in the amount of source gas used can be achieved.

To model the reactor the flow of gases through porous media was studied theoretically and experimentally and transport equations were developed that describe the overall flux of the gas - either single component or binary mixture - through the pores in terms of the molecular parameters and the pore characteristcs. These flux equations were developed based on our understanding of the various collision mechanisms that contribute to the flow at low pressures as described by the kinetic theory of ideal gases and are applicable to the whole low pressure region - Knudsen, transition, and viscous regimes - without need of any adjustment of the parameters of the model when the equations are applied to a pressure range where more than one mechanism contributes to the flow or there is a transition from one contributing mechanism to another along that range.

Using the equations developed, modeling of the reactor was presented for various porois frit configurations and for several typical reacting schemes used in the semiconductor industry.

Finally, construction of a reactor based on the novel principle has been completed and some flow visualization experiments were performed to observe actual gas flow patterns. From these experiments it was concluded that when the porous solids are present at the inlet and outlet of the reactor, the flow is considerably better distributed along the radial direction and that should result in better deposition uniformity.

Thin film depositiopn experiments need to be performed to evaluate the performance of this reactor.

a) Hot-wall, non-epitaxial deposition of silicon with three or four wafers placed on a rack next to each other parallel to the reactant flow to determine the thickness uniformity of the deposited film from wafer to wafer. In addition, depositions should should be performed under the same conditions with a reactor without frits to compare the perfoprmance of the fritted reactor. Typical conditions would be 600°C temperature and 1 Torr pressure with a flow rate of 500 sccm of 3% SiH_2Cl_2 (dichlorosilane) in N_2.

b) Cold-wall deposition of epitaxial material. A barrel type susceptor needs to be fabricated for this case. Preferred mode of heating is radiant heating beacause of the better temperature uniformity achieved throughout the susceptor. An alternate geometry is to machine a flat susceptor holding two or three wafers and position the susceptor in such a way that the center line of the susceptor is alligned with the center axial line of the reactor. Typical conditions are 920°C tempereature and 2 Torr pressure with a flow rate of 500 sccm of 3% SiH_2Cl_2in N_2. These experiments need to be performed in reactors with and without frits. In addition, the above experiments ought to be done with varying flow rates to determine the minimum flow rate needed for uniform deposition in the chamber to compare the amounts needed in the cases with and without frits.

One item of concern that needs to be mentioned is reactions in which gas phase nucleation occurs. This normally happens at hot wall conditions where the temperature of the gas is uniform, but it may also happen during cold wall conditions since there is a temperature gradient over the hot susceptor and the wall temperature reaches 400 to 500°C due to radiation. A very commonly used gas that nucleates is silane. When gas phase nucleation occurs, there is a possibility that the outlet pores will plug . In such a case, this reactor may not be recommended because it will be difficult to maintain the pressure in the deposition section at the desired level and frequent shut down will be necessary to unplug the pores. An additional case where pore plugging may occur is when due to conduction the frit temperature rises and consequently there might be some deposition on the pores with subsequent pore blocking occuring. In such a case, cooling of the frit is needed with air blowing or a wate circulating coil wrapped around the outlet section of the reactor.

REFERENCES

Adzumi, H., Bull. Chem. Soc. Japan, 12 (1937) 292, 304.

Adzumi, H., Bull. Chem. Soc. Japan, 14 (1939) 343.

Arnell, J.C., and Hennenberry, G.O., Can. J. Res., A26 (1948) 29.

Barrer, R.M., and Barrie, R.A., Proc. Roy. Soc., A213 (1952) 250.

Barrer, R.M., and Grove, D.M., Trans. Far. Soc., 47 (1951) 826.

Bloem, J., J. Cryst. Gr., 50 (1980) 581.

Carman, P.C., and Allen, J.C., Can. J. Res., A26 (1948) 128.

Carman, P.C., Proc. Roy. Soc., A203 (1950) 55.

Carman, P.C., "Flow of Gases through Porous Media," Academic Press, New York (1956).

Chapman, S., and Cowling, T.G., "The Mathematical Theory of Non-Uniform Gases," University Press, Cambridge (1970).

Cunningham, R.E., and Williams, R.J.J., "diffusion in Gases and Porous Media," Plenum Press, New York (1980).

Fahien, R.W., "Fundamentals of Transport Phenomena," McGraw-Hill, New York (1983).

Grove, D.M., and Ford, M.G., Nature, 182 (1958) 999.

Gunn, R.D., and King, C.J., A.I.Ch.E. J., 15 (1969) 507.

Hiby, J.W., and Pahl, M., Z. Naturf., 7a (1952) 542.

Knudsen, M., Ann. Phys.,. 28 (1909) 75.

Lea, F.M., and Nurse, R.W., "Symposium on Particle Size Analysis, I.Ch.E. and S.C.I.," 4February1947 p. 47.

Lee, H.H., "Heterogeneous Reactor Design," Butterworths, Boston (1985).

Levine, I.N., "Physical Chemistry," McGraw-Hill, New York, (1978).

Mason, E.A., Evans III, R.B., and Watson, G.M., J. Chem. Phys., 38 (1963) 1808.

Pollard, W.G., and Present, R.D., Phys. Rev., 73 (1948) 762.

Reid, R.C., Prausnitz, J.M., and Sherwood, T.K., "The Properties of Gases and Liquids," McGraw-Hill, New York (1977).

Rigden P.H., Nature, 157 (1946) 268, 694.

Rigden, P.H., J. Soc. Chem. Ind., 66 (1947) 130.

Schwertz, F.A., J. Appl. Phys., 20 (1949) 1070.

Sze, S.M., ed., "VLSI Technology," McGraw-Hill, New York (1988).

Wallick, G.C., and Aronofsky, J.S., Petr. Trans., 201 (1954) 322.

Westphal, G.H., J. Cryst. Gr., 65 (1983) 105.

BIOGRAPHICAL SKETCH

Elias Stassinos was born in Athens, Greece, on September 30, 1959. He graduated from the A Prototype High School of Athens in 1977, and he came to the United States to study chemical engineering. He received his B.S. degree Magna Cum Laude from Youngstown State University in Ohio in June 1982. He then moved to Gainesville to attend graduate school at the University of Florida. He received his M.S. degree in chemical engineering in August 1983, and continued for his Ph.D. under Dr. Hong H. Lee. After completion of his studies, he plans to pursue a teaching and research career in the academia.

I certify that I have read this study and that in my opinion it conforms to acceptable standards of scholarly presentation and is fully adequate, in scope and quality, as a dissertation for the degree of Doctor of Philosophy.

Hong H. Lee, Chairman
Professor of Chemical Engineering

I certify that I have read this study and that in my opinion it conforms to acceptable standards of scholarly presentation and is fully adequate, in scope and quality, as a dissertation for the degree of Doctor of Philosophy.

Ray W. Fahien

Ray W. Fahien
Professor of Chemical Engineering

I certify that I have read this study and that in my opinion it conforms to acceptable standards of scholarly presentation and is fully adequate, in scope and quality, as a dissertation for the degree of Doctor of Philosophy.

Gar B. Hoflund

Gar Hoflund
Professor of Chemical Engineering

I certify that I have read this study and that in my opinion it conforms to acceptable standards of scholarly presentation and is fully adequate, in scope and quality, as a dissertation for the degree of Doctor of Philosophy.

Spyros A. Svoronos

Spyros A. Svoronos
Associate Professor of Chemical
Engineering

I certify that I have read this study and that in my opinion it conforms to acceptable standards of scholarly presentation and is fully adequate, in scope and quality, as a dissertation for the degree of Doctor of Philosophy.

Pete S Zory

Peter S. Zory
Professor of Electrical
Engineering

This dissertation was submitted to the Graduate Faculty of the College of Engineering and to the Graduate School and was accepted as partial fulfillment of the requirements for the degree of Doctor of Philosophy.

August, 1989

Dean, College of Engineering

Dean, Graduate School